Closed Form Displacement Solutions for Circumferentially Cracked Pipes in Bending and Tension

UM-MEAM-88-06

S. H. Yoo and J. Pan

October 10, 1988

Closed Form Displacement Solutions for Circumferentially Cracked Pipes in Bending and Tension

UM-MEAM-88-06

S. H. Yoo and J. Pan
Mechanical Engineering and Applied Mechanics
The University of Michigan
Ann Arbor, Michigan 48109

Abstract

Sanders' axial and normal displacement solutions are examined for two different geometries and loads : (a) an infinite long pipe containing a circumferential crack in bending and tension, and (b) a semi-infinite long pipe containing a circumferential crack at the fixed end in bending and tension. A parabolic approximation of the axial displacement solutions for the cracked pipes is given for calculation of the crack opening area for leak-rate evaluation.

1. Introduction

Although there are many available research results on the stress intensity factors and energy-release rates for circumferentially cracked pipe in bending and tension [1,2], few displacement solutions are available in the literature. Within the context of shell theories, the axial displacement solutions can be used to evaluate the leak rates of the cracked pipes containing pressurized fluids. The normal displacement solutions, on the other hand, can be used to evaluate the moment carrying capacity of the cracked pipe when finite deformation of the pipe is considered. Therefore, we examined the closed form expressions of the axial and normal displacement solutions developed by Sanders and Alabi [3-7] in this report for two different geometries and loads: (a) an infinite long pipe containing a circumferential crack in bending [3,4] and tension [5], and (b) a semi-infinite long pipe containing a circumferential crack at the fixed end in bending [6] and tension [7], as schematically shown in Figure 1(a) and 1(b). Figure 1(c) shows the schematic plot of the pipe cross section containing a circumferential crack. In the figure, R represents the pipe mean radius, t represents the wall thickness, and 2α represents the total crack angle.

As the effects of transverse shear strain are found to be significant [8] only for a very short crack where $\alpha = O(\epsilon^2)$, the first approximation theory which is consistent with the Kirchoff hypotheses are valid for finite crack problems. Here ϵ is a small dimensionless parameter defined as

$$\epsilon^2 = \frac{t}{\sqrt{12(1-\nu^2)}R} \tag{1}$$

where ν is Poisson's ratio. In Sanders' equation, the complex displacements and stress functions of a pipe are given by two charateristic functions [5]. The total solution consists of a nominal solution from each remote loading, an elementary solution, a semi-membrane solution and an edge-effect solution. The physical displacements are calculated by taking the real parts of the complex displacements from Sanders' solutions for the two characteristic functions. The simplification procedures in these semi-membrane solutions produce errors no greater than those due to the use of the classical thin shell theory for $R/t \leq 30$.

2. An Infinite Long Pipe with a Circumferential Crack in Bending and Tension

2.1 The Bending Case

Energy-release rate solutions for the combined bending and tension loading case were given in reference [4] and more elaborate results for tension loading were given in [5]. The expressions for the axial displacement u and the normal displacement w for bending loading were derived by Sanders [3]. These dimensionless variables are related to the physical axial and normal displacement, U and W, by

$$U = \frac{\sigma R}{E} u \tag{2}$$

$$W = \frac{\sigma R}{E\epsilon^2} w \tag{3}$$

where σ is the nominal stress, E is Young's modulus. In this bending case, the nominal stress σ is defined as:

$$\sigma = \frac{M}{\pi R^2 t} = \frac{MR}{I} \tag{4}$$

where M is the remote bending moment, and I is the moment of inertia of the circular cross section. The following constants depending only on the pipe geometry were obtained by Sanders [3] as:

$$\Delta = -\frac{\pi}{\sqrt{2}} \cos\alpha$$

$$P = \frac{\alpha - \frac{1}{2}\sin 2\alpha}{\sin\alpha \cos\frac{\pi-\alpha}{\sqrt{2}} + \sqrt{2}\cos\alpha \sin\frac{\pi-\alpha}{\sqrt{2}}}$$

$$A = \cos\alpha - \sqrt{2}B - \frac{1}{2}P\cos\frac{\pi-\alpha}{\sqrt{2}}$$

$$B = -\frac{1}{2\sqrt{2}\pi}P(\sqrt{2}\sin\frac{\pi-\alpha}{\sqrt{2}} + \alpha\cos\frac{\pi-\alpha}{\sqrt{2}}) - \frac{1}{\sqrt{2}\pi}(\sin\alpha - \alpha\cos\alpha) \tag{5}$$

$$\Delta C = \frac{\sqrt{2}}{4}P\cos\frac{\pi-\alpha}{\sqrt{2}}(\pi - \alpha + \frac{1}{2}\sin 2\alpha) + \frac{\sqrt{2}}{4}[\alpha(\alpha-\pi)\sin\alpha + 4\pi\cos\alpha$$

$$+\frac{5}{4}(2\alpha - \sin 2\alpha)\cos\alpha]$$

$$\Delta D = (2\alpha - \sin 2\alpha)(\frac{1}{8}P\cos\frac{\pi-\alpha}{\sqrt{2}} - \frac{5}{16}\cos\alpha) - \frac{1}{4}\alpha^2\sin\alpha\,.$$

Then the axial displacement u and the normal displacement w can be expressed in terms of the quantities defined above as:

$$u = \begin{cases} \epsilon^{-1}\{-B + D\cos\theta + \frac{\sqrt{2}}{2}(-A + C\cos\theta + 3\cos\theta - \frac{1}{2}\theta\sin\theta)\} & \text{on the crack ;} \\ 0 & \text{off the crack ,} \end{cases} \tag{6}$$

$$w = \begin{cases} (2+C)\cos\theta - \frac{1}{2}\theta\sin\theta & \text{on the crack ;} \\ -\sqrt{2}D\cos\theta - \frac{1}{2}P\cos\frac{\pi-\theta}{\sqrt{2}} & \text{off the crack .} \end{cases} \tag{7}$$

In Figure 2, the undeformed circular cross sections of the pipes are shown by the dotted lines and the deformed shapes of the cross section containing the crack are shown by the solid lines for $\alpha = 10°, 30°, 60°$ and $90°$ based on the normal displacement solutions of equation (7). All the normal displacement solutions shown are normalized such that the maximum values of the θ-variation w are set at 10% of the radius R of the undeformed cross section. For the cases shown, the pipe becomes "taller" under remote bending. When finite deformation of the pipe is accounted for, this deformed shape tends to increase the bending stiffness of the cracked pipe. The same kinds of ovalization were observed from the experiments of Kanninen et al. [9] and Bruckner et al. [10] for circumferentially cracked pipes with relatively large cracks. When the crack becomes small, in these experiments, the cracked pipe deforms into a shape such that the pipe is "shorter". This "shorter" deformed shape agrees with the pre-buckling mode of a pipe of elastic-plastic materials [11].

In Figure 3, the values of the axial displacement u normalized by u_M, which is the maximum axial displacement at $\theta = 0$, are plotted as the functions of the normalized θ by α for $\alpha = 10°, 30°, 60°$ and $90°$. Note that the maximum displacement u_M at $\theta = 0$ can be calculated easily from equations (5) and (6) as:

$$u_M = \frac{\sqrt{2}}{4}\epsilon^{-1}\{\alpha\tan\alpha + (1-\cos\alpha)(2 - \frac{\alpha\sec^2\alpha - \tan\alpha}{\tan\alpha + \sqrt{2}\tan\frac{\pi-\alpha}{\sqrt{2}}})\}\,. \tag{8}$$

As shown in the figure, the four curves are remarkably close each other. When α is less than $60°$, the opening profile can be fitted almost exactly by a parabolic curve which is

the solid line shown in the figure. When α is larger than 60°, for example 90°, as shown in the figure, the solution still can be conservatively approximated by the parabolic curve. The detail of the curve fitting will be discussed in Section 4, but we can asymptotically calculate the values of u_M and u as $\alpha \to 0$ (and consequently $\theta \to 0$). The second order expansions of u_M and u have the simple expressions as:

$$u_M = \frac{\sqrt{2}}{2}\epsilon^{-1}\alpha^2 \tag{9}$$

$$u = \epsilon^{-1}\left(\frac{\sqrt{2}}{2}\alpha^2 - \frac{\sqrt{2}}{2}\theta^2\right). \tag{10}$$

Combining equations (9) and (10) yields a parabolic equation as:

$$\frac{u}{u_M} = 1 - \left(\frac{\theta}{\alpha}\right)^2. \tag{11}$$

This is the equation plotted as solid lines in Figure 3 and the subsequent plots of the axial displacement solutions.

2.2 The Tension Case

The displacement solutions for an infinite long pipe with a circumferential crack under remote tension are given here based on the work in reference [5]. In the tension loading case, σ is the tensile stress in the pipe at infinity. The following quantities which were dependent only upon the pipe geometry were defined by Sanders [5] as:

$$\Delta = \sin\alpha\cos\frac{\pi-\alpha}{\sqrt{2}} + \sqrt{2}\cos\alpha\sin\frac{\pi-\alpha}{\sqrt{2}}$$

$$\beta = \sin\frac{\pi-\alpha}{\sqrt{2}} + \frac{\alpha}{\sqrt{2}}\cos\frac{\pi-\alpha}{\sqrt{2}}$$

$$\Delta P = 2(\sin\alpha - \alpha\cos\alpha)$$

$$\pi A = \frac{1}{3}\alpha^3 - \frac{\pi}{2}\alpha^2 + \frac{\sqrt{2}}{2}\left[\sin\frac{\pi-\alpha}{\sqrt{2}} - \left(\frac{\pi-\alpha}{\sqrt{2}}\right)\cos\frac{\pi-\alpha}{\sqrt{2}}\right]P \tag{12}$$

$$2\pi B = -\left(\frac{\sqrt{2}}{3}\alpha^3 + \beta P\right)$$

$$\Delta C = \sqrt{2}(\beta - \Delta D)$$

$$2\pi\Delta D = (\sin 2\alpha - 2\alpha\cos 2\alpha)\sin\frac{\pi-\alpha}{\sqrt{2}} + \sqrt{2}(\alpha^2 + 2\sin^2\alpha$$
$$-3\alpha\sin\alpha\cos\alpha)\cos\frac{\pi-\alpha}{\sqrt{2}}$$

Then the axial displacement u and the normal displacement w can be expressed in terms of these quantities as:

$$u = \begin{cases} -\epsilon^{-1}\{\frac{\sqrt{2}}{2}(1 - C\cos\theta + \frac{1}{2}\theta^2 + A) + B - D\cos\theta\} & \text{on the crack ;} \\ 0 & \text{off the crack} \end{cases} \tag{13}$$

$$w = \begin{cases} -1 + C\cos\theta & \text{on the crack ;} \\ -\sqrt{2}D\cos\theta - \frac{1}{2}P\cos\frac{\pi-\theta}{\sqrt{2}} & \text{off the crack .} \end{cases} \tag{14}$$

The deformed shapes of the cross section are shown in Figure 4 for $\alpha = 10°, 30°, 60°$ and $90°$ based on the normal displacement solution of equation (13). The deformed shapes are slightly different from those of the bending case and show the same type of ovalization effects. The normalized axial displacements are shown in Figure 5. The shapes are slightly closer to the asymptotic solid line than the bending case. The maximum displacement u_M is expressed as:

$$u_M = \frac{\sqrt{2}}{4}\epsilon^{-1}\{\alpha^2 + 2\frac{1-\cos\alpha}{\cos\alpha}\frac{\alpha + \sqrt{2}\tan\frac{\pi-\alpha}{\sqrt{2}}}{\tan\alpha + \sqrt{2}\tan\frac{\pi-\alpha}{\sqrt{2}}}\}. \tag{15}$$

The asymptotic limits of u_M and u as $\alpha \to 0$ are the same as equations (9) and (10) and consequently equation (11) can be used for approximation.

3. A Semi-infinite Long Pipe with a Circumferential Crack at the Fixed End in Bending and Tension

Energy-release rate solutions were given for this configuration by Alabi and Sanders [7]. The complete results for the bending case were given in Alabi [6]. It was reported that the proximity of the fixed boundary had an alleviating effect on energy-release rates.

3.1 The Bending Case

The necessary constants for the displacement solutions were given by Alabi [6] as:

$$A = \frac{\alpha - \cos\alpha \sin\alpha}{\sqrt{2}\cos\alpha \sin\frac{\alpha}{\sqrt{2}} - \sin\alpha\cos\frac{\alpha}{\sqrt{2}}}$$

$$B = \frac{\alpha - \cos\alpha \sin\alpha}{\sqrt{2}\cos\alpha \sin\frac{\pi-\alpha}{\sqrt{2}} + \sin\alpha\cos\frac{\pi-\alpha}{\sqrt{2}}}$$

$$\pi a_I = \alpha\cos\alpha - \sin\alpha + A(\frac{\alpha}{2}\cos\frac{\alpha}{\sqrt{2}} - \frac{1}{\sqrt{2}}\sin\frac{\alpha}{\sqrt{2}})$$

$$2\sqrt{2}\pi b_R = \alpha\cos\alpha - \sin\alpha + \pi a_I - B(\frac{1}{\sqrt{2}}\sin\frac{\pi-\alpha}{\sqrt{2}} + \frac{\alpha}{\sqrt{2}}\cos\frac{\pi-\alpha}{\sqrt{2}})$$

$$a_R = \cos\alpha - 2\sqrt{2}b_R + a_I - \frac{B}{2}\cos\frac{\pi-\alpha}{\sqrt{2}}$$

$$2\sqrt{2}b_I = -a_R - a_I + \cos\alpha + \frac{A}{2}\cos\frac{\alpha}{\sqrt{2}} \tag{16}$$

$$\frac{\pi}{2}c_I\sin\alpha = a_R\sin^2\alpha - \frac{1}{4}(\alpha + \cos\alpha\sin\alpha)(3\sin\alpha + \alpha\cos\alpha) + \frac{\alpha}{8}\sin\alpha(4 + \cos 2\alpha)$$

$$+\frac{3}{8}\cos\alpha\sin^2\alpha + 2\sqrt{2}b_I\sin^2\alpha + a_I\sin^2\alpha + A\Gamma$$

$$\pi\sqrt{2}d_R\sin\alpha = \pi c_I\sin\alpha + (-2a_I - 2\sqrt{2}b_I + 2\sqrt{2}b_R)\sin^2\alpha + B\Delta - A\Gamma$$

$$c_R\cos\alpha = -2\cos\alpha + \frac{1}{2}\alpha\sin\alpha + c_I\cos\alpha - 2\sqrt{2}d_R\cos\alpha - \frac{B}{2}\cos\frac{\pi-\alpha}{\sqrt{2}}$$

$$2\sqrt{2}d_I\cos\alpha = -2\cos\alpha + \frac{1}{2}\alpha\sin\alpha - c_R\cos\alpha - c_I\cos\alpha + \frac{A}{2}\cos\frac{\alpha}{\sqrt{2}}$$

$$\Gamma = -2\sin^2\alpha\cos\frac{\alpha}{\sqrt{2}} + \frac{1}{2\sqrt{2}}\sin\frac{\alpha}{\sqrt{2}}(\alpha + 5\cos\alpha\sin\alpha)$$

$$\Delta = 2\sin^2\alpha\cos\frac{\pi-\alpha}{\sqrt{2}} + \frac{1}{2\sqrt{2}}\sin\frac{\pi-\alpha}{\sqrt{2}}(\alpha + 5\cos\alpha\sin\alpha)\,.$$

The displacement solutions are expressed in terms of the above quantities as:

$$u = \epsilon^{-1}\{-b_R - b_I + (d_R + d_I)\cos\theta + \frac{\sqrt{2}}{2}(-a_R + c_R\cos\theta - \frac{1}{2}\theta\sin\theta + 3\cos\theta)\} \tag{17}$$

$$w = -\frac{1}{2}\theta\sin\theta + (c_R + c_I + 2 + 2\sqrt{2}d_I)\cos\theta - \frac{A}{2}\cos\frac{\theta}{\sqrt{2}}\,. \tag{18}$$

Figure 6 shows the deformed shapes of the cross section for $\alpha = 10°, 30°, 60°$ and $90°$ based on the normal displacement solution of equation (18). As the boundary is fixed, the normal displacements appear only on the pipe part. It is clear that the pipe becomes "taller" under remote bending loads. The axial displacement solutions are shown in Figure 7. The shapes for smaller cracks are closer to to the solid line which is the plot of equation (11). The maximum displacement u_M is expressed (from equations (16) and (17)) as:

$$u_M = \frac{\sqrt{2}}{4}\epsilon^{-1}\{\alpha\tan\alpha+(1-\cos\alpha)[2-\frac{1}{2}(\frac{\alpha\sec^2\alpha-\tan\alpha}{\sqrt{2}\tan\frac{\pi-\alpha}{\sqrt{2}}+\tan\alpha}-\frac{\alpha\sec^2\alpha-\tan\alpha}{\sqrt{2}\tan\frac{\alpha}{\sqrt{2}}-\tan\alpha})] \quad (19)$$

The asymptotic limits of u_M and u as $\alpha \to 0$ can be obtained easily from equations (17) and (19) as:

$$u_M = \frac{\sqrt{2}}{4}\epsilon^{-1}\alpha^2 \quad (20)$$

$$u = \epsilon^{-1}\left(\frac{\sqrt{2}}{4}\alpha^2 - \frac{\sqrt{2}}{4}\theta^2\right). \quad (21)$$

Although the values are half of the values for the infinite long pipes, the same parabolic approximation is possible and consequently equation (11) holds for this case also.

3.2 The Tension Case

The necessary constants for the displacement solutions were given by Alabi and Sanders [7] as:

$$A = \frac{\sin\alpha-\alpha\cos\alpha}{\frac{1}{\sqrt{2}}\cos\alpha\sin\frac{\alpha}{\sqrt{2}}-\frac{1}{2}\sin\alpha\cos\frac{\alpha}{\sqrt{2}}}$$

$$B = \frac{\sin\alpha-\alpha\cos\alpha}{\frac{1}{\sqrt{2}}\cos\alpha\sin\frac{\pi-\alpha}{\sqrt{2}}+\frac{1}{2}\sin\alpha\cos\frac{\pi-\alpha}{\sqrt{2}}}$$

$$\pi a_I = -\frac{1}{3}\alpha^3 + A(\frac{\alpha}{2}\cos\frac{\alpha}{\sqrt{2}} - \frac{1}{\sqrt{2}}\sin\frac{\alpha}{\sqrt{2}})$$

$$2\sqrt{2}\pi b_R = -\frac{1}{3}\alpha^3 + \pi a_I - B(\frac{\alpha}{2}\cos\frac{\pi-\alpha}{\sqrt{2}} + \frac{1}{\sqrt{2}}\sin\frac{\pi-\alpha}{\sqrt{2}})$$

$$a_R = -\frac{1}{2}\alpha^2 - 2\sqrt{2}b_R + a_I - \frac{B}{2}\cos\frac{\pi-\alpha}{\sqrt{2}}$$

$$2\sqrt{2}b_I = -\frac{1}{2}\alpha^2 - a_R - a_I + \frac{A}{2}\cos\frac{\alpha}{\sqrt{2}} \tag{22}$$

$$\frac{\pi}{2}c_I \sin\alpha = \{a_R + \frac{1}{2}(\alpha^2 - 4) + 2\sqrt{2}b_I + a_I\}\sin^2\alpha + \frac{\alpha}{2}(\alpha + 3\cos\alpha\sin\alpha) + A\Gamma$$

$$\pi\sqrt{2}d_R \sin\alpha = \pi c_I \sin\alpha + (-2a_I - 2\sqrt{2}b_I + 2\sqrt{2}b_R)\sin^2\alpha + B\Delta - A\Gamma$$

$$c_R \cos\alpha = 1 + c_I \cos\alpha - 2\sqrt{2}d_R \cos\alpha - \frac{B}{2}\cos\frac{\pi - \alpha}{\sqrt{2}}$$

$$2\sqrt{2}d_I \cos\alpha = 1 - c_R \cos\alpha + \frac{A}{2}\cos\frac{\alpha}{\sqrt{2}} - c_I \cos\alpha$$

$$\Gamma = -2\sin^2\alpha\cos\frac{\alpha}{\sqrt{2}} + \frac{1}{2\sqrt{2}}\sin\frac{\alpha}{\sqrt{2}}(\alpha + 5\cos\alpha\sin\alpha)$$

$$\Delta = 2\sin^2\alpha\cos\frac{\pi - \alpha}{\sqrt{2}} + \frac{1}{2\sqrt{2}}\sin\frac{\pi - \alpha}{\sqrt{2}}(\alpha + 5\cos\alpha\sin\alpha)$$

The displacement solutions are expressed in terms of the above quantities as:

$$u = \epsilon^{-1}\{-b_R - b_I + (d_R + d_I)\cos\theta + \frac{\sqrt{2}}{2}(-1 - \frac{1}{2}\theta^2 - a_R + c_R\cos\theta)\} \tag{23}$$

$$w = -1 + (c_R + c_I)\cos\theta + 2\sqrt{2}d_I\cos\theta - \frac{A}{2}\cos\frac{\theta}{\sqrt{2}}. \tag{24}$$

Figure 8 shows the deformed shapes of the cross section for $\alpha = 10°, 30°, 60°$ and $90°$ based on the normal displacement solutions of equation (24). It is clear that the pipe becomes "shorter" under remote tensile loads as α becomes large. This ovalization effect is opposite to the other cases. The axial displacement solutions are shown in Figure 9, in which all three lines except for $\alpha = 90°$ are close to the solid line which is the plot of equation (11). The maximum displacement u_M is expressed (from equations (22) and (23)) as:

$$u_M = \frac{\sqrt{2}}{4}\epsilon^{-1}\{\alpha^2 + \frac{1 - \cos\alpha}{\cos\alpha}[2 - \frac{\tan\alpha - \alpha}{\sqrt{2}\tan\frac{\pi-\alpha}{\sqrt{2}} + \tan\alpha} + \frac{\tan\alpha - \alpha}{\sqrt{2}\tan\frac{\alpha}{\sqrt{2}} - \tan\alpha}]\}. \tag{25}$$

The asymptotic limits of u_M and u as $\alpha \to 0$ turn out as the same as equations (9) and (10). Consequently, equation (11) holds for this case also.

4. Discussions

In terms of energy-release rates and stress intensity factors, Sanders' solutions were compared well with the finite element results of Forman et al. [12]. For the calculation of the crack opening areas in pipes, Wüthrich [13] discussed several different methods and presented some analytical formulae based on the solutions given by Erdogan and Kibler [14]. But those solutions are good only for short cracks because the shallow shell thoery is used. But simple expressions which are valid even for large cracks are possible for the axial displacement and the opening area. As previously derived, equation (11) serves as the asymptotic limit for the four cases as $\alpha \to 0$. The area under this curve, $A_\circ$, as $\alpha \to 0$ becomes $\frac{2}{3}$ which is one quarter of the total opening area for the infinitely long pipe and one half of the total opening area for the semi-infinite pipe with a fixed end. To check the validity of the above equation, all the axial displacement solutions were approximated by the parabolic equations:

$$\frac{u}{u_M} = c(\frac{\theta}{\alpha})^2 - (c+1)\frac{\theta}{\alpha} + 1. \tag{26}$$

The area under each parabolic approximation, $A_\circ$, and the parameter c are listed in Table 1 for the four cases. It is shown that the values of c approach -1 asymptotically.

The areas are smaller than $\frac{2}{3}$ at the most by 7% for all the cases studied. Therefore equation (11) is a good conservative approximation of the axial displacement solutions for leak rate calculations. The real physical opening area, A, can be approximately calculated for an infinite long pipe as:

$$A = \frac{8}{3} R^2 \alpha u_M \frac{\sigma}{E} \tag{27}$$

and for a semi-infinite long pipe as:

$$A = \frac{4}{3} R^2 \alpha u_M \frac{\sigma}{E} \tag{28}$$

These results may be useful to check numerical or experimental results in the linear elastic region since these solutions are not accounted for plastic effects.

Acknowledgements

This report was prepared with the support of the U.S. Nuclear Regulatory Commission (NRC) under Grant No. NRC-04-87-113. The authors thank very much to Professor Sanders for providing his unpublished note. Helpful discussions with the program manager Mike Mayfield is greatly appreciated.

References

1. Wilkowski, G. M. (ed.), *Circumferential Cracks in Pressure Vessels and Piping*, PVP-Vol. 94 and 95, ASME, New York, 1983.

2. Sih, G. C. (ed.), " Plates and Shells with Cracks," *Mechanics of Fracture 3*, Noordhoff, Leyden, The Netherlands, 1977.

3. Sanders, J. L., Jr., Private communication, 1988.

4. Sanders, J. L., Jr., "Circumferential Through-Crack in a Cylindrical Shell Under Combined Bending and Tension," Transactions of the ASME, *Journal of Applied Mechanics*, Vol. 50, No. 1, 1983, pp. 221.

5. Sanders, J. L., Jr., "Circumferential Through-Crack in a Cylindrical Shell Under Tension," Transactions of the ASME, *Journal of Applied Mechanics*, Vol. 49, No. 1, 1983, pp. 103-107.

6. Alabi, J. L., "Circumferential Cracks in Cylindrical Shells," Ph.D. Thesis, Harvard University, Cambridge, Massachusetts, 1984.

7. Alabi, J. L. and Sanders, J. L., Jr., "Circumferential Crack at the Fixed End of a Pipe," *Engineering Fracture Mechanics*, Vol. 22, No. 4, 1985, pp. 609-616.

8. Simmonds, J. G. and Duva, J., "Thickness effects are Minor in the Energy-Release Rate Integral for Bent Plates Containing Elliptic Holes or Cracks," Transactions of the

ASME, *Journal of Applied Mechanics*, Vol. 48, No. 1, 1981, pp. 320-326.

9. Kanninen, M. F., Zahoor, A., Wilkowski, G., Abou-Sayed, I., Marcshall, C., Broek, D., Sampath, S., Rhee, H. and Ahmad, J., "Instability Predictions for Circumferentially Cracked Type-304 Stainless Steel Pipes Under Dynamic Loading," EPRI NP-2347, Vols. 1 and 2, Electric Power Research Institute, Palo Alto, Calif., Apr. 1982.

10. Bruckner, A., Grunmach, R., Kneifel, B. Munz, D. and Thun. G., "Fracture of Pipes with Through-Wall Circumferential Cracks in Four-Point Bending," *Circumferential Cracks in Pressure Vessels and Piping*, Edited by Wilkowski, G. M., PVP-Vol. 95, ASME, New York, 1983, pp. 123-136.

11. Tang, S. C., Chu, C. C., and Yeung, K. S., "Collapse of Long, Noncircular, Cylindrical Shells under Pure Bending," *Computers & Structures*, Vol. 21, No. 6, 1985, pp. 1345-1353.

12. Forman, R. G., Hickman, J. C. and Shivarkumar, V., "Stress Intensity Factors for Circumferential Through Cracks in Hollow Cylinders Subjected to Combined Tension and Bending Loads," *Engineering Fracture Mechanics*, Vol. 21, No. 3, 1985, pp. 563-571.

13. Wüthrich, C., "Crack Opening Areas in Pressure Vessels and Pipes," *Engineering Fracture Mechanics*, Vol. 18, No. 5, 1983, pp. 1049-1057.

14. Erdogan, F. and Kibler, J. J., "Cylindrical and Spherical Shells with Cracks," *Int. J. Fracture Mechanics*, Vol. 5, 1969, pp. 229-237.

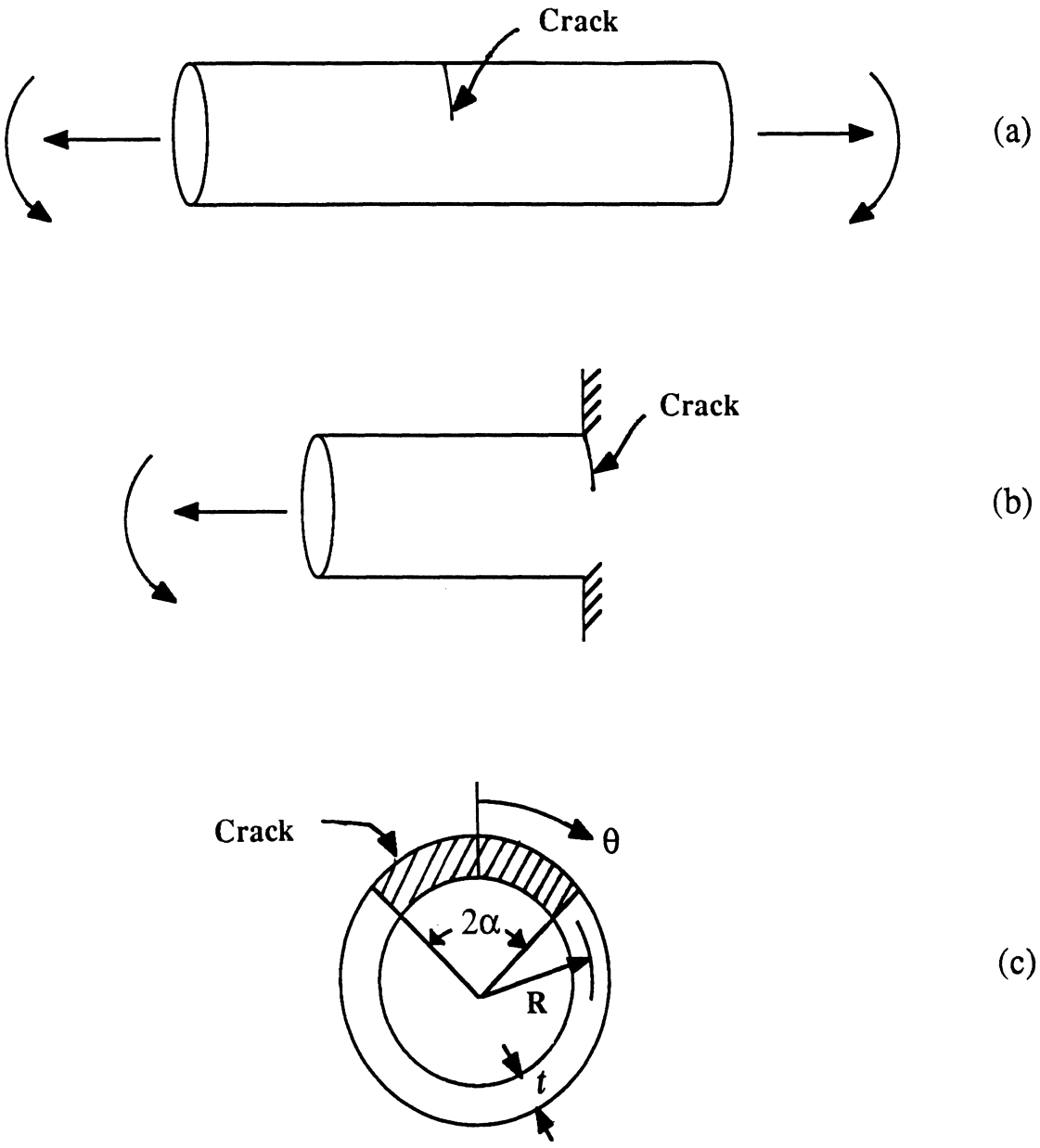

Figure 1 Circumferentially cracked pipes

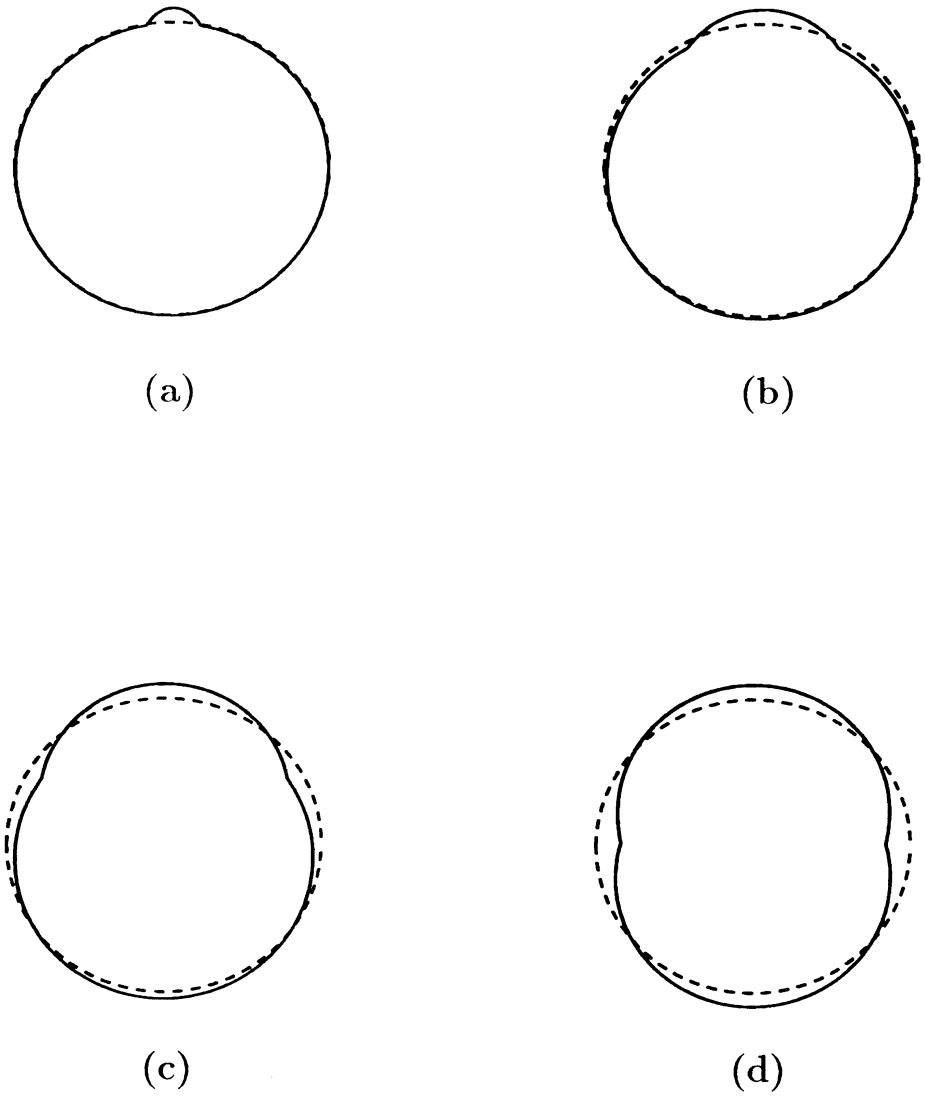

Figure 2 Normalized normal displacements of an infinite long pipe with a circumferential crack subjected to remote bending. (a) $\alpha = 10^\circ$ (b) $\alpha = 30^\circ$ (c) $\alpha = 60^\circ$ (d) $\alpha = 90^\circ$

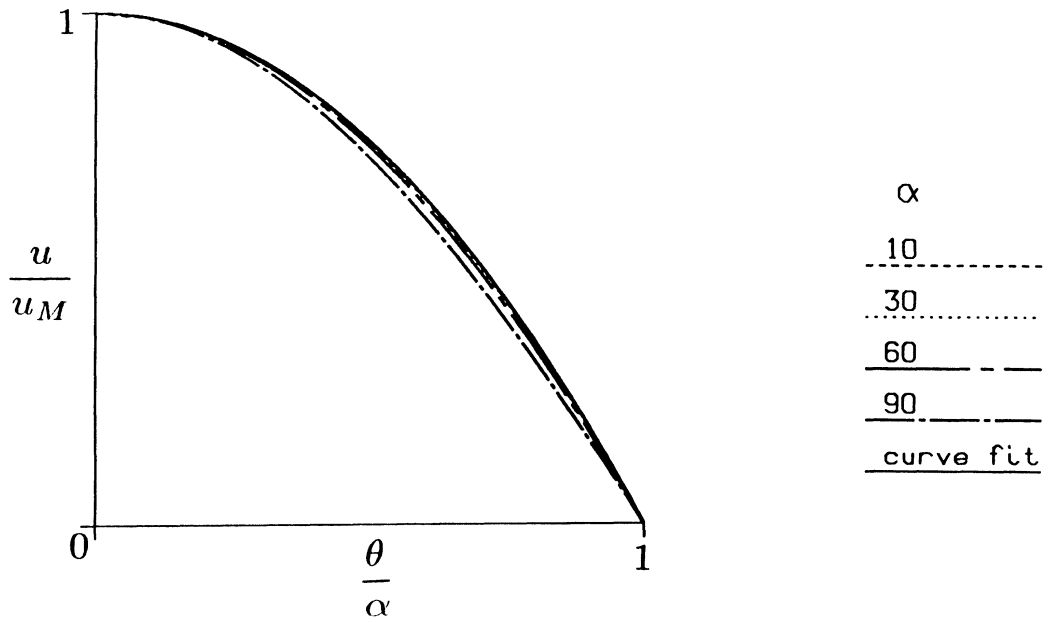

Figure 3 Normalized axial displacements of an infinite long pipe with a circumferential crack subjected to remote bending.

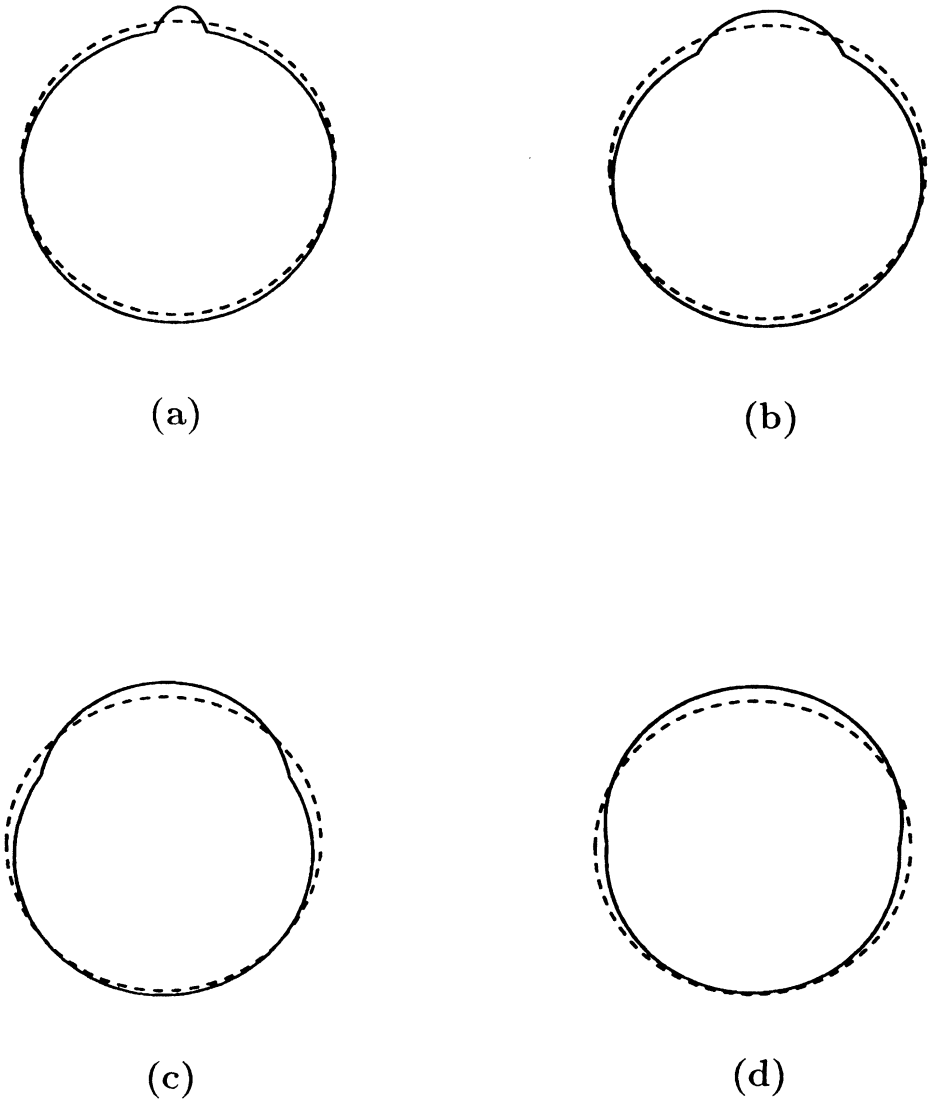

Figure 4 Normalized normal displacements of an infinite long pipe with a circumferential crack subjected to uniform remote tension.
(a) $\alpha = 10^\circ$ (b) $\alpha = 30^\circ$ (c) $\alpha = 60^\circ$ (d) $\alpha = 90^\circ$

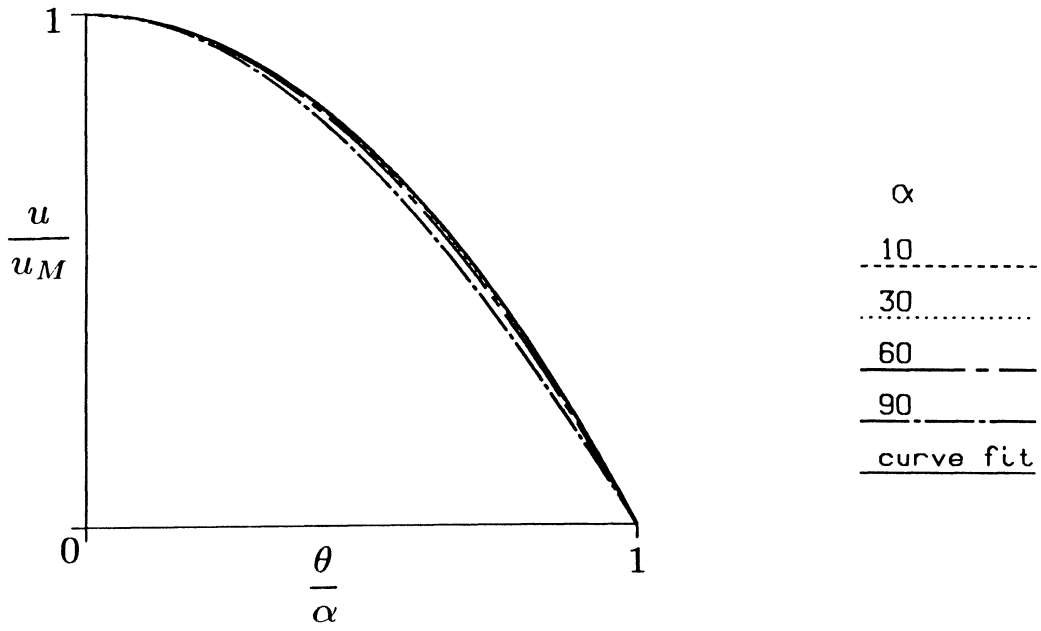

Figure 5 Normalized axial displacements of an infinite long pipe with a circumferential crack subjected to uniform remote tension.

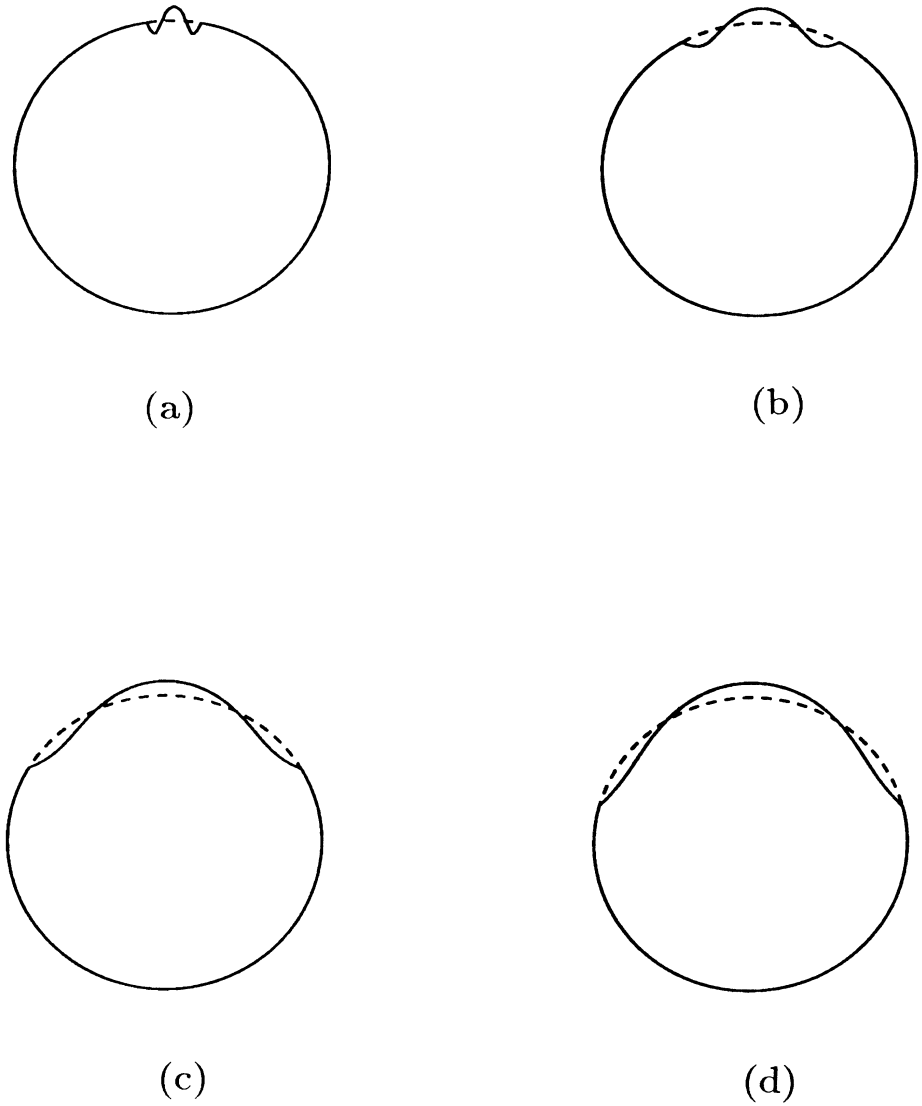

Figure 6 Normalized normal displacements of a semi–infinite long pipe with a circumferential crack at the fixed end subjected to remote bending.
(a) $\alpha = 10^\circ$ (b) $\alpha = 30^\circ$ (c) $\alpha = 60^\circ$ (d) $\alpha = 90^\circ$

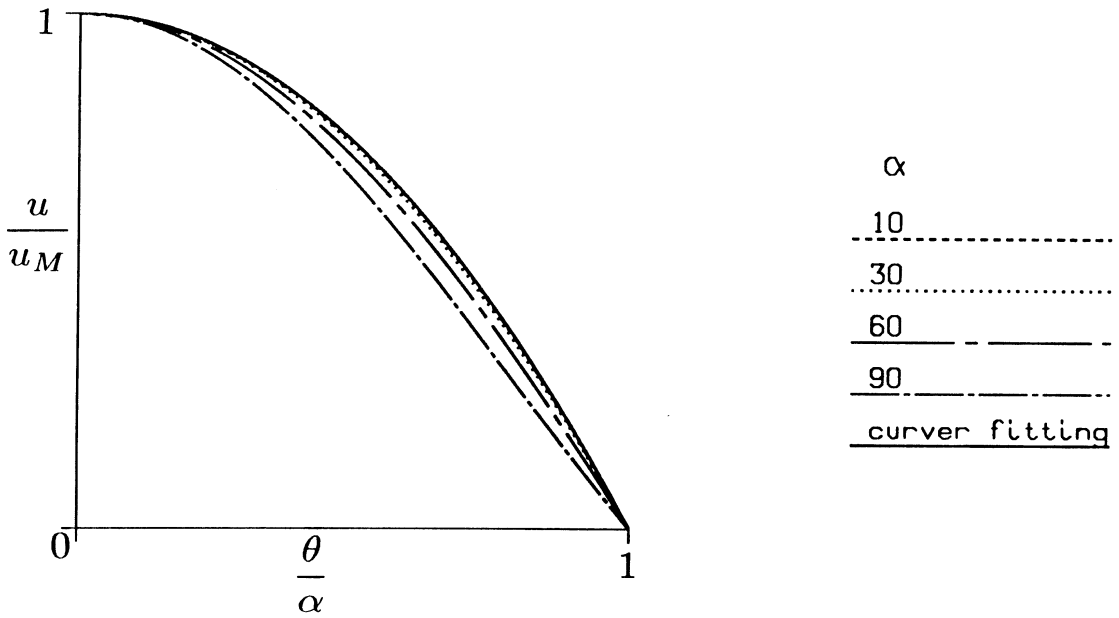

Figure 7 Normalized axial displacements of a semi–infinite long pipe with a circumferential crack at the fixed end subjected to remote bending.

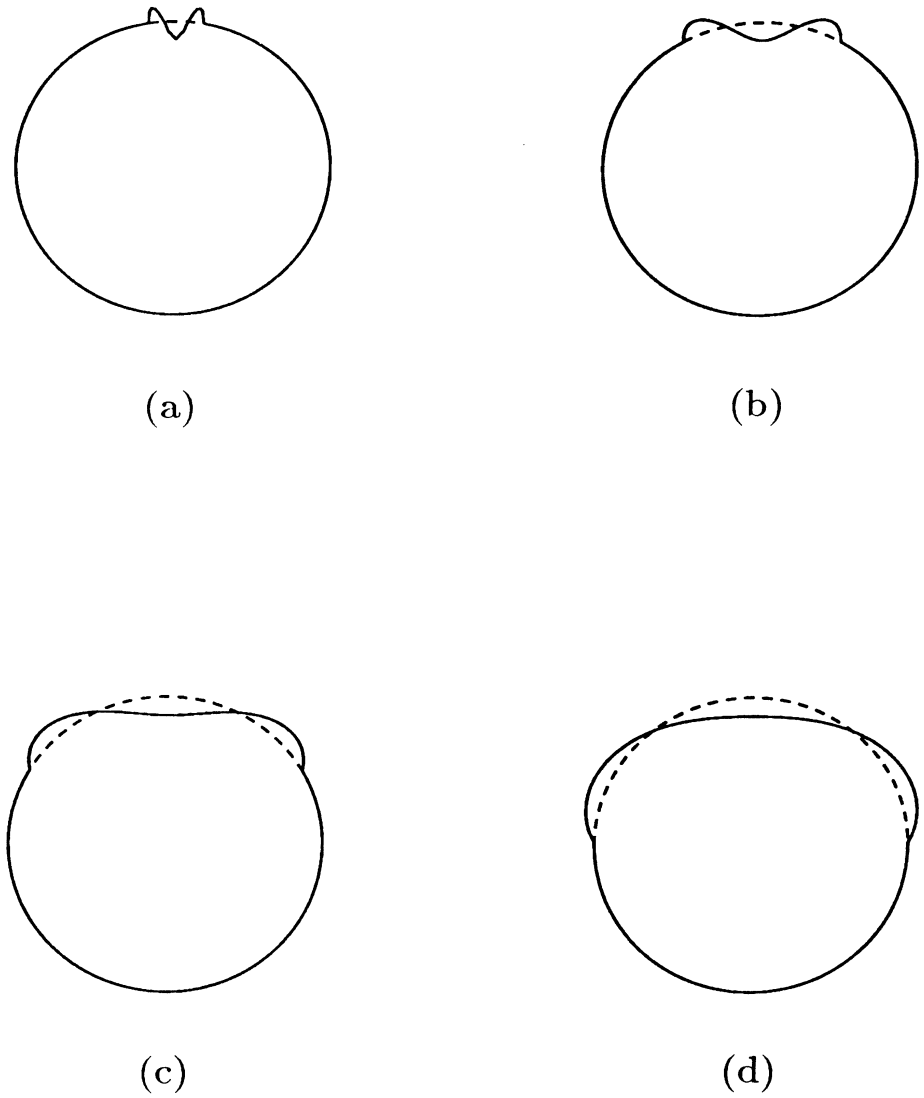

Figure 8 Normalized normal displacements of a semi–infinite long pipe with a circumferential crack at the fixed end subjected to uniform remote tension. (a) $\alpha = 10^\circ$ (b) $\alpha = 30^\circ$ (c) $\alpha = 60^\circ$ (d) $\alpha = 90^\circ$

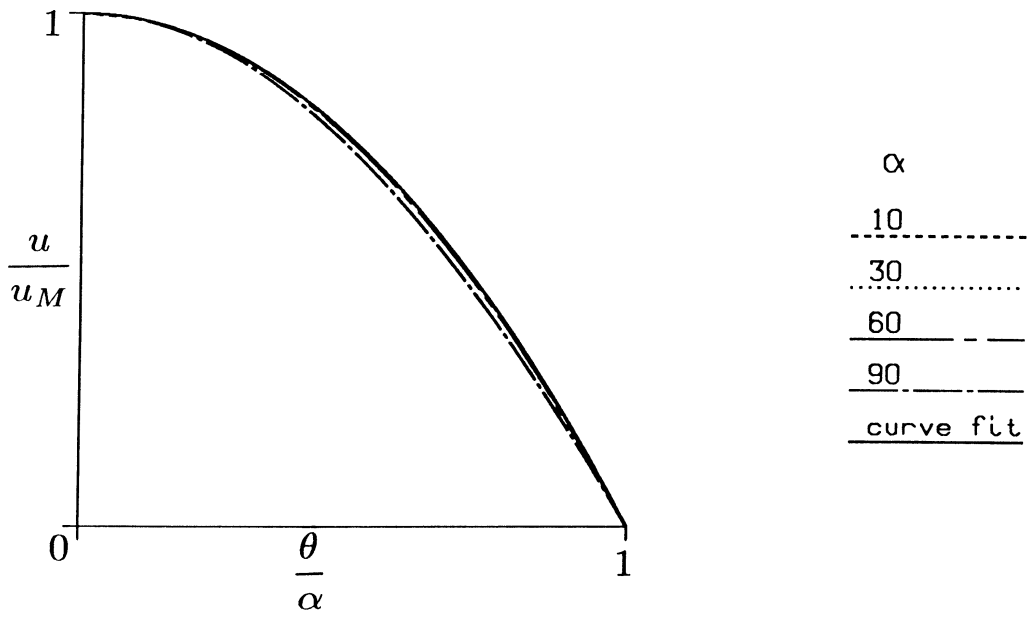

Figure 9 Normalized axial displacements of a semi–infinite long pipe with a circumferential crack at the fixed end subjected to uniform remote tension.

α	Ao	c
10	0.666	-0.997
30	0.662	-0.975
60	0.649	-0.901
90	0.630	-0.794

(a)

α	Ao	c
10	0.667	-0.999
30	0.665	-0.991
60	0.659	-0.954
90	0.644	-0.872

(b)

α	Ao	c
10	0.666	-0.996
30	0.661	-0.966
60	0.644	-0.874
90	0.623	-0.753

(c)

α	Ao	c
10	0.667	-1.000
30	0.666	-0.999
60	0.663	-0.981
90	0.652	-0.916

(d)

Table 1 Crack opening area Ao and curve fitting parameter c for
(a) an infinite long pipe in bending, (b) an infinite long pipe in tension,
(c) a semi-infinite long pipe with a fixed end in bending and
(d) a semi-infinite long pipe with a fixed end in tension.